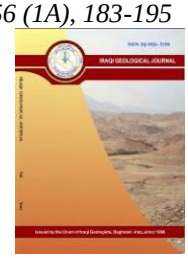
Iraqi Geological Journal

Journal homepage: https://www.igj-iraq.org



Joint Analysis of InSAR, ERT, and in-Situ Geological Survey in Landslide Prone Area: A Case in Laeya Village, North Buton Regency, Indonesia

Jamhir Safani[1,*], Golok Jaya[2], Fitra Saleh[3], Ali Okto[1], Suryawan Afsar[1], and Jahidin Lania[1]

[1] Department of Geophisical Engineering, Faculty of Earth Sciences and Technology, Universitas Halu Oleo, Kendari, Indonesia
[2] Department of Informatics Engineering, Faculty of Engineering, Universitas Halu Oleo, Kendari, Indonesia
[3] Department of Geography, Faculty of Earth Sciences and Technology, Universitas Halu Oleo, Kendari, Indonesia
* **Correspondence**: jamhir.safani@uho.ac.id

Received:
16 July 2022

Accepted:
28 September 2022

Published:
31 January 2023

Abstract

Landslide investigation in Laeya Village of North Buton Regency, Indonesia, is necessary since this area is frequently experiencing landslides. In this study, we applied a joint analysis of interferometric synthetic aperture radar (InSAR), electrical resistivity tomography (ERT), and in-situ geology observation. The objectives of this multidisciplinary study are: a) to estimate ground deformation through the InSAR method, b) estimation of subsurface characteristics based on the electrical resistivity of rocks, as well as estimation of the shape of the slip plane and the type of landslide that resulted; and c) to identify the surface geology conditions of the site from an in-situ geology survey. The InSAR data of the Sentinel-1A acquired from 2015 to 2017 were processed using the Sentinel toolbox. The resistivity data collected utilizing the electrodes array of the Wenner-Schlumberger configuration were processed employing the RES2DINV. The in-situ geology survey involving the observation of elevation, slope, and soil and rock type was also carried out in the landslide area. The InSAR method may estimate the deformation of slope material of the investigated sites with a magnitude ranging from -53 mm to +55 mm. The negative mark of the magnitude means that the ground deformation is ground subsidence and the positive means ground uplift. The ERT method has successfully estimated the existence of the saturated zones, the clay layer that acts as a slip plane, and the slip surface type. There are at least two types of slip planes estimated, namely the planar and uneven curvature slip planes that generate the translational and the complex landslides, respectively. In-situ observations of geological conditions support the results obtained from the InSAR and ERT methods.

Keywords: InSAR; ERT; In-situ geology; Landslide; Slip plane

1. Introduction

North Buton Regency, Southeast Sulawesi Province, Indonesia, is a region that is experiencing many landslides. During the peak of rain in May and June 2017, landslide disasters struck four villages, including Laeya Village. Statistical data from the BPBDS of North Buton Regency shows that landslides in 2017 resulted in 12 houses being damaged, one person being killed, and one person being injured. This incident is not the first event of landslides. Previous landslides have even occurred in 2013 and 2016 (BPBD North Buton Regency, 2018).

DOI:10.46717/igj.56.1A.14ms-2023-1-26

Many researchers, such as Jongmans et al. (2009), Borrelli et al. (2014), Wang et al. (2015), Uhlemann et al. (2015), Schlogel et al. (2015); Hu and Shan (2016), Szalai et al. (2017), Czikhardt et al. (2017), Virk et al. (2018); Falae et al. (2019), Necula et al. (2021); Ayele and Cherie (2021), Yan et al. (2022), have carried out landslide investigation using the monodisciplinary approach of geophysics (like ERT, seismic surface wave, seismic refraction, and ground penetrating radar- GPR), geology (like geological, geomorphological, and hydrogeological survey) and remote sensing (like optical-, radar satellite, and airborne imagery)**.** The monodisciplinary approach of non-invasive geophysical techniques provides subsurface characteristics across depth and delineates geometry of the probable sliding surface of the landslide areas (Falae et al., 2019). In studying landslides, Jongmans et al. (2009) utilized five geophysical methods, namely seismic noise measurement, resistivity tomography, P-wave seismic refraction, S-wave seismic refraction, and surface wave inversion, combined with borehole data, that demonstrated how the seismic and electrical profiles correlate with geotechnical data and geomorphological observations. Wang et al. (2015) also joined the surface wave seismic method (MASW) and microtremor array for the analysis of the stability of a landslide dam. Hu and Shan (2016) and Yan et al. (2022) joined the electrical resistivity and GPR methods, and these integrations were able to delineate the probable slip plane of landslides. Therefore, geophysical methods, including resistivity methods, are the common-used method of estimating the properties of the rock layers and the geometry models of the slip plane.

Utilization of one of the remote sensing techniques, namely Synthetic Aperture Radar Interferometry (InSAR) is also increasingly popular for monitoring road damage (Murdzek et al., 2018; Jaya et al., 2020), and for analysis of land subsidence (Zhou et al., 2017), as well as for imaging of tectonic deformation (Fattahi, 2015). InSAR allows detection of ground movement rates with high accuracy, which is in millimeters per year (Czikhardt et al., 2017; Zhou et al., 2017; Murdzek et al., 2018; Necula et al., 2021; Ayele and Cherie, 2021).

A multidisciplinary approach by joining several measurement methods may provide comprehensive information on potential landslides in an area (Giocoli et al., 2015). It will overcome the problem of ambiguity of interpretation that usually occurs in an individual approach. The InSAR technique can provide an accurate depiction of the landslide surface mechanism for a more global area (Schlogel et al., 2015; Czikhardt et al., 2017; Virk et al., 2018; Necula et al., 2021; Ayele and Cherie, 2021), even though the measurements are made far above the Earth's surface. On the other hand, geophysical methods such as ERT can be carried out on the surface of the Earth with a more efficient cost and time, and provide more local information about subsurface characteristics (i.e. electrical resistivity properties of soils and rocks) and geometric models of sliding surfaces (Perrone et al., 2006; Bellanova et al., 2016; Kannaujiya et al., 2019). So, this geophysical study simultaneously strengthens the information obtained from the InSAR technique carried out far above the Earth's surface. Perrone et al. (2006), Kannaujiya et al. (2019), and Rauff et al. (2020) conducted a joint analysis of InSAR and ERS and deduced that this integration may remedy the understanding of both the surface and subsurface mechanisms.

Although the studies of the subsurface characteristics and mechanisms in landslide-prone areas have been carried out and published by many authors, as mentioned above, the studies that discuss the shapes of the sliding surfaces and how they relate to the resulting type of sliding movement have not been widely reported. The types of sliding surfaces (such as translational, rotational, and complex sliding planes) greatly affect the movement mechanism of landslide material, and thus influence the classification of landslide types (Hungr et al., 2013). Therefore, this study discusses the estimation of the shape of the sliding plane from the geophysical approach (i.e., ERT) and its relationship to the resulting type of landslide. These geophysical measurements were carried out in several selected areas where ground deformations occurred referring to the InSAR data. Furthermore, in-situ observations will further confirm the results of the InSAR and ESR methods through direct observations and

measurements of the parameters that affect landslides such as elevation, slope, soil and rock types, and distance from the road (Tuncel et al., 2021; Ayele and Cherie, 2021).

The targets to be achieved through this multidisciplinary study are: (a) estimation of the ground deformation through the InSAR approach; (b) estimation of subsurface characteristics based on the electrical resistivity of rocks, as well as estimation of the shape of the slip plane and the type of landslide that resulted; and (c) depiction of geological conditions of the research area from in situ geology survey to confirm the results from the two previous approaches.

2. Geological Setting of the Study Area

The study area is located in Buton Island. This location has undergone several tectonic processes from the pre-Eocene to the Oligocene. The tectonic process resulted in the emergence of many folds and faults with non-uniform directions (Davidson, 1991; Sikumbang et al., 1995).

From the morphological aspect, the research area consists of mountain ranges that are slightly curved in the north-south direction. Steep mountains dominate the morphological system developed in the study area, but a few plains also exist that are currently used as settlements. The steep mountains have slopes ranging from 15% to 70% (or 8.53° to 35°) and are even very steep at more than 70% (or 35°) (Fig. 1a). Areas with such slopes have the potential to experience landslides, especially if there is a thick layer of unconsolidated weathering material over an impermeable layer.

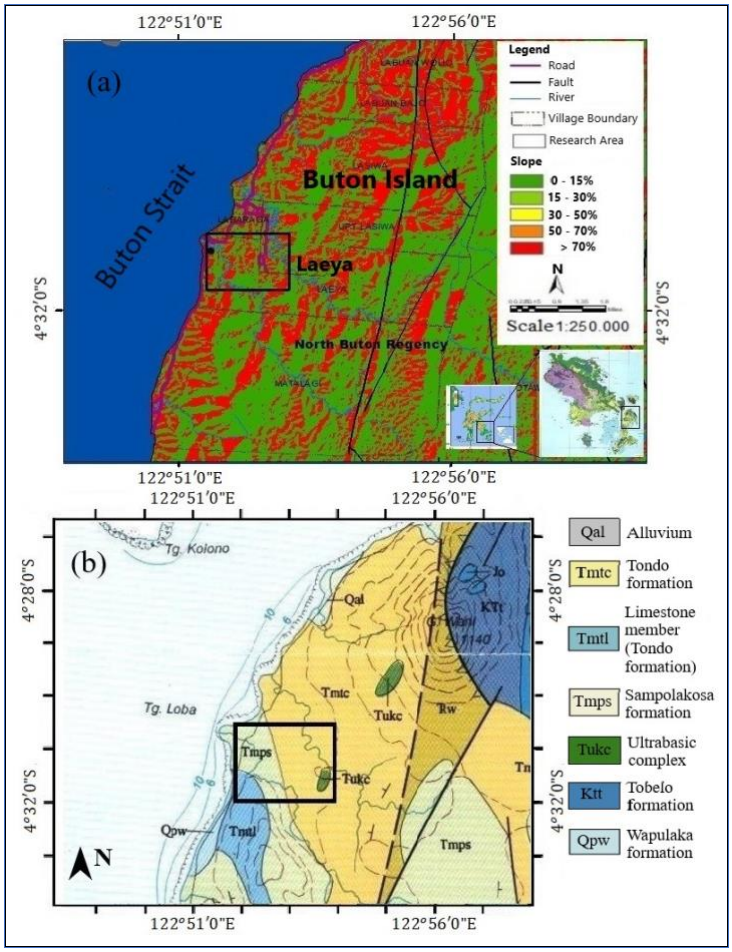


Fig. 1. (a) Topography, and (b) geological map surrounding the study area in North Buton Regency, Indonesia, adopted from Davidson (1991) and Sikumbang et al. (1995). The study area signed with the black block.

The rock units that make up the research area are grouped into Mesozoic and Cenozoic rocks. The Mesozoic rock group has a Triassic to Upper Cretaceous age, while the Cenozoic rock group is Miocene and Pleistocene (Davidson, 1991). Fig. 1b shows that the study area is dominated by the Tondo and Sampolakosa Formation formations. The Tondo Formation is composed of sedimentary rocks such as conglomerate, gravel sandstone, and sandstone with the insertion of siltstone, siltstone, and clay. Meanwhile, the Sampolakosa Formation consists of marl and calcarenite limestones. In several locations, calcarenite limestones that have undergone the early stages of the metamorphic process emerge. The metamorphic process is indicated by the change in color and texture of the limestone to blackish gray with a more compact rock texture, which is commonly referred to as meta-limestone.

Landslides occur frequently in study areas and have resulted in damage to public housing, deaths, and injuries. These landslide events left traces such as scarps, heads, and undisturbed soil outcrops. The traces of these landslides, together with the shape of sliding surfaces estimated from the ESR method, will be used to evaluate the resulting type of landslides, whether rotational, translational, or complex translational landslides.

3. Landslide Classification

The classification of landslide types designed by Varnes (1978) has become the most commonly utilized classification in the past four decades. Varnes's material division (including rock, debris, and earth), which is one of the most essential factors in devising landslide classification, is, however, incompatible with accepted geotechnical and geological terminology of rocks and soils (Hungr et al., 2013). A modification to the Varnes classification was proposed by Hungr et al. (2013) based on the following two aspects: first, modification of the definition of landslide-forming material to conform to the accepted geotechnical and geological terminology; second, several changes related to movement mechanisms (Highland and Bobrowsky, 2008; Hungr et al., 2013).

The movement mechanisms describe the actual internal mechanics of how the landslide mass is displaced: fall, topple, slide, spread, or flow (Highland and Bobrowsky, 2008; Hungr et al., 2013). In this research, we deal with one of the movement types, which is the slide. There are three types of slide movements that are often encountered in the field, involving rotational, translational/planar, and complex/multiple rotational slides (Fig. 2) (Highland and Bobrowsky, 2008; Hungr et al., 2013; Schlögel et al., 2015).

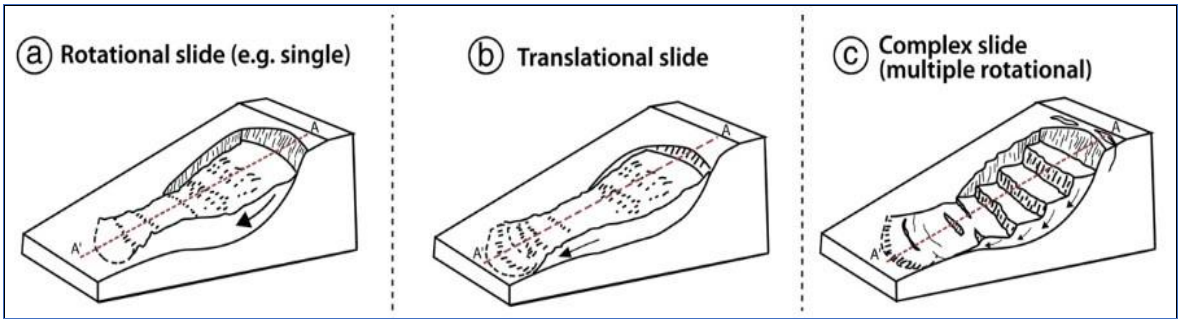


Fig. 2. Three dimensional view of the slope morphology: (a) rotational slide with a single curvature sliding surface; (b) translational slide with a nearly planar sliding surface; and (c) compound/ complex slide with a series of embedded curvature sliding surface (Schlögel et al., 2015)

The rotational landslide (Fig. 2a) is a landslide in which the surface of rupture is curved upward (spoon-shaped) and the slide movement is more or less rotational about an axis that is parallel to the contour of the slope. The displaced mass may, under certain circumstances, move as a relatively coherent mass along the rupture surface with little internal deformation. The head of the displaced

material may move almost vertically downward, and the upper surface of the displaced material may tilt backwards toward the scarp. This type of movement is associated with slopes ranging from about 20° to 40° (Highland and Bobrowsky, 2008).

A translational or planar landslide (Fig. 2b) is the sliding of cohesive materials on an inclined planar sliding plane. The head of the displaced materials separates from stable soil along a deep tension crack. Meanwhile, a complex slide (Fig. 2c) is characterized by a slip surface consisting of several planes or a surface of uneven curvature and the presence of many secondary heads and minor scarps in the moving body (Hungr et al., 2013).

4. Materials and Methods

4.1. Data Acquisition

We conducted the investigation using three joint approaches, namely remote sensing, geophysics, and in-situ geology survey. The remote sensing approach utilized InSAR data to identify the ground deformation. The geophysical investigations were carried out by employing the ERT measurement to estimate subsurface conditions, involving the electrical resistivity values and the geometrical shape of the slip surface. The in-situ geology survey involved measurements of elevation and slope of the investigated site, and collections of soil and rock data outcropped around the site to supply information on the surface geology and geomorphology conditions of the investigated area.

The InSAR data used in this work are those acquired by Sentinel-1A, which is the first satellite launched by the European Space Agency (ESA) in 2014. There are several reasons for using this Sentinel-1A. First, in carrying out its mission, this satellite carries an instrument that is able to collect data in all weather, namely C-band synthetic-aperture radar (SAR). This instrument may collect data day or night with a 12-day return cycle, so that revisits of the target area can be done quite often and allows for updating data assimilation (Lievens et al., 2011). Second, the image data acquired by the Sentinel-1A have been successfully used for landslide monitoring and evaluation in various parts of the world (Schlogel et al., 2015; Czikhardt et al., 2017; Virk et al., 2018; Necula et al., 2021; Ayele and Cherie, 2021). Third, the image data cover worldwide and can be accessed free of charge by all users without limitations. When data collections are performed, the Sentinel-1A satellite operates in interferometric wide (IW) mode by crossing the area of interest from north to south in the descending pass direction and from south to north in the ascending pass direction (Rauff et al., 2020).

The InSAR analysis was carried out over the research area by utilizing the available dataset, which formed of a single look complex (SLC). The InSAR data acquired on 26th April 2015 and 9th May 2017 from ascending track were incorporated. These two acquired Sentinel-1A images acted as a master and slave pair, respectively. Table 1 provides characteristics of the Sentinel-1A dataset, which involves acquisition mode, frequency, product type, frame, absolute orbit, orbit track, polarization, and date of acquisition. These InSAR data were obtained from https://vertex.daac.asf.alaska.edu.

Table 1. Characteristics of Sentinel-1A dataset

File Name	Characteristics	
S1A_IW_SLC_1SSV_20150426T212648_ 20150426T212717_005660_007426_0207 (Master image)	Acquisition mode	Interferometric Wide (IW)
	Center frequency	5.405 GHz
	Product type	Single Look Complex (SLC)
	Frame	7426
	Absolute orbit	5660
	Orbit track	Ascending
	Polarization	VV
	Acquisition date	26th April 2015
S1A_IW_SLC_1SDV_20170509T212656_ 20170509T212723_016510_01B5DC_ 33CB_6 (Slave image)	Acquisition mode	Interferometric Wide (IW)
	Center frequency	5.405 GHz
	Product type	Single Look Complex (SLC)
	Frame	1B5DC
	Absolute orbit	16510
	Orbit track	Ascending
	Polarization	VV + HV
	Acquisition Date	9th May 2017

Measurements by the ERT method were carried out at three profile lines, labeled Line-1, Line-2, and Line-3 in Fig. 3. All ERT profile lines have a north-south direction, parallel to the hill-slope. In determining the location of the ERT profile lines, we set the following criteria: first, being in a residential area prone to landslides; second, being near the main road. Both criteria are essential in landslide vulnerability assessment (Galli and Guzzetti, 2007). ERT data collection was conducted when the electrical current was inserted into the ground through the current electrodes, and the potential difference was measured through the potential electrodes. Collections of the ERT data employed a Syscal Pro instrument equipped with 22 electrodes, consisting of two potential electrodes and 20 current electrodes. The electrode arrangement applied the Wenner-Schlumberger configuration with the distance between the adjacent electrodes at 3 m; thus, the length of each ERT profile line of the 20 current electrodes used is 60 m. We utilized the Wenner-Schlumberger configuration due to its high sensitivity of this configuration to the horizontal and vertical changes and its higher signal-to-noise ratio than other configurations (Fressard et al., 2016; Bellanova et al., 2016; Falae et al., 2019).



Fig. 3. Measurements using the ERT method divided into three lines (i.e. Line-1, Line-2, and Line-3); All lines having a north-south direction and facing the road.

In the landslide area, geology data collections involving the elevation, slope, and soil and rock types were also carried out. Measurements of the electrode elevations employed the GPS required to ensure the topographic influence on the generated electrical resistivity model. Investigations of soil and rock types were carried out by directly observing the landslide materials and the undisturbed soil/ rock outcrops near the landslide area. This is necessary to ensure the presence of the layer that may act as a slip plane of the landslide. The slope measurement utilized the geology compass of Brunton Type. This in-situ geology survey was performed to complete the landslide analysis obtained from the InSAR and geophysical investigations.

4.2. Data Processing

The basis of InSAR data collection is a measure of the phase difference between two acquisitions. Here, the InSAR data were processed for the detection of ground deformation through Differential Interferometry (DInSAR) (Perrone et al., 2006; Ayele and Cherie, 2021) using the Sentinel toolbox, which is the free open-source software. The steps of the InSAR data processing are shown in Fig. 4. There were at least six steps in the data processing: first, splitting the image into the area of interest; second, coregistration to form interferogram formation from a pair of SLC images, namely master and slave images; third, topography phase removal/flattening was to flatten the interferogram model to the Earth projection; fourth, phase filtering to remove temporal decorrelation, geometric decorrelation, volume scattering, and processing error; and fifth, phase unwrapping was then conducted to remove aliasing error, i.e., the shifting of the high frequency of the wave becoming lower. The last step was a transformation from phase to ground deformation and terrain correction for providing geometric representation, so the picture resembles the truth (Jaya et al., 2019).

The measured electrical potential and the electrical current inserted to the ground through the current electrodes were processed to present the measured apparent resistivity. The inversion algorithm of Res2DInv (Loke et al., 2020) was utilized to derive a two-dimensional (2-D) section of the electrical resistivity tomography (ERT). This algorithm works based on a smoothness-constrained least-square method by minimizing misfit between measured- and calculated apparent resistivity values.

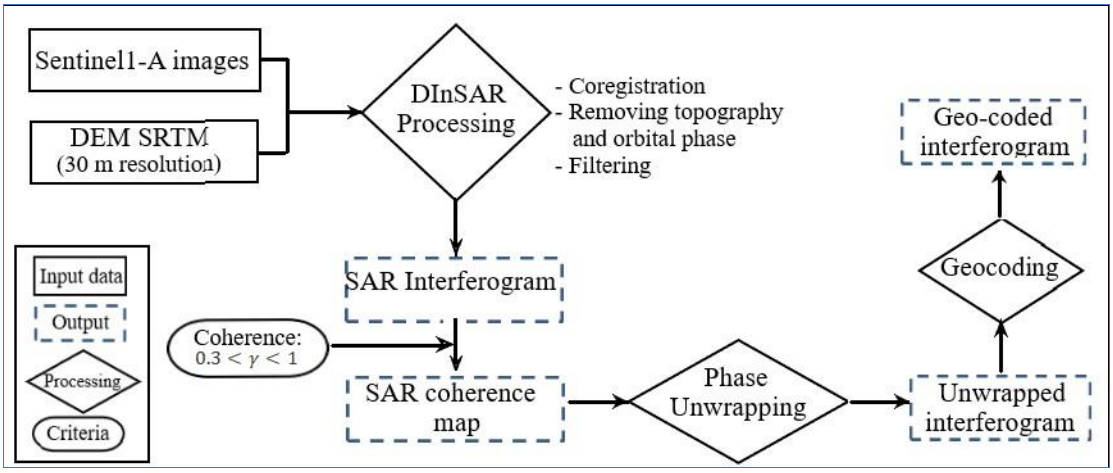


Fig. 4. Methodological flowchart used for processing Sentinel1-A dat

5. Results and Discussions

In the DInSAR processing stage, DEM SRTM data were used to eliminate errors from topographic effects, so that the interferogram projection plane becomes a flat plane. In this process, we provided a coherence criterion that shows the identicality of the image pair, where the greater the coherence value, the more identical the image pair. The minimum coherence criterion given to generate the interferogram

was 0.3, as used by many authors, such as Schlögel et al. (2015) and Ayele and Cherie (2021). The final stage of this process is to provide a geo-coded interferogram that represents a map of ground deformations in the study area.

Fig. 5 displays ground deformation with a magnitude ranging from -53 to +55 mm derived from the InSAR data processing by using the data acquired in 2015 and 2017. The negative mark of the magnitude means that the ground deformation is land subsidence and the positive means land uplift. So the maximum land subsidence and land uplift that occurred in the study area are 53 mm and 55 mm, respectively. Several locations were experiencing maximum land subsidence, as shown by the red circle in Fig. 5. Fortunately, the maximum land subsidence (i.e., 53 mm) is relatively far from the residential locations and main roads.

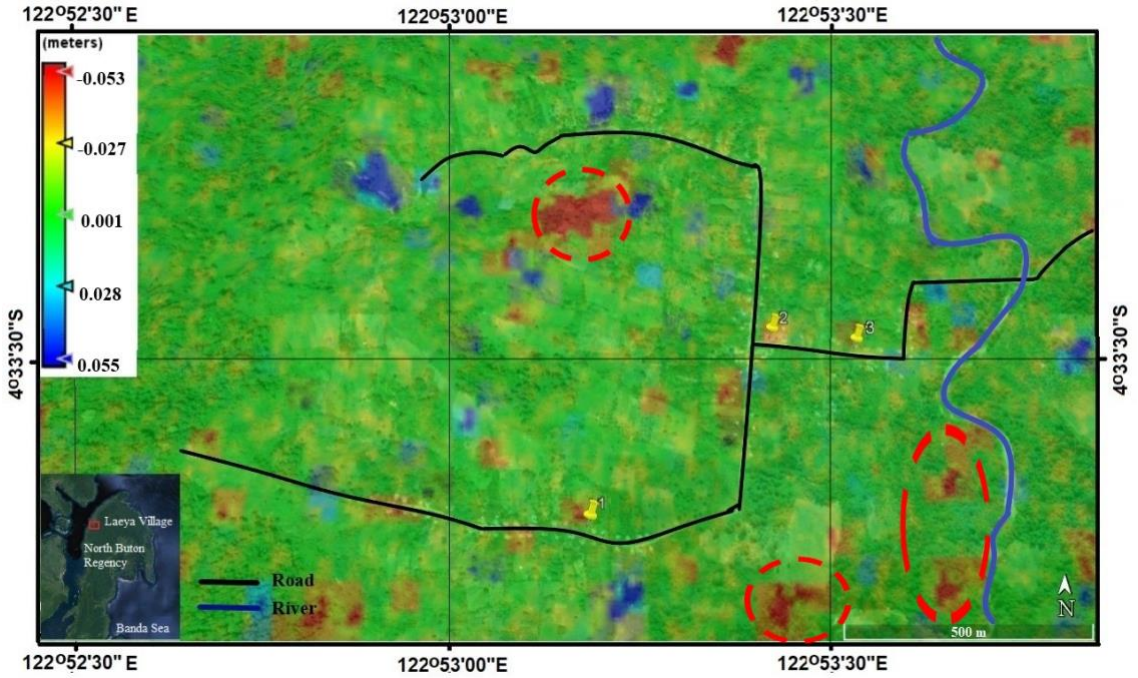


Fig. 5. Ground movement of the research area in Laeya Village, North Buton Regency of Indonesia, resulted from InSAR data acquired from 2015 to 2017. The "yellow spikes" represent land subsidence around settlements and main roads.

However, several locations around the settlements and main roads were experiencing land subsidence, as shown by the "yellow spikes" in Fig. 5, although with a smaller magnitude (i.e., around 40 mm). This slow deformation and together with the cracking of surficial ground materials on a steep hillside could be the initial potential for landslides (Hungr et al., 2013). Therefore, in-situ surveys to inspect the geological conditions that affect landslides, such as geophysical and geological surveys, are essential. At the three yellow spikes in Fig. 5, ERT and in-situ geological surveys were carried out. These spikes coincide with the ERT profile lines as shown in Fig. 3.

The 2-D sections of ERT for line-1, line-2, and line-3 are shown in Figs. 6a, 6b, and 6c, respectively. All these inversion results considered the topographic effect on each model. Determination of the topographic effects utilized the elevation data measured at each profile line. In Line-1, the minimum elevation is 95 m above mean sea level (m.s.l.), which is at the first electrode of the electrical current and the maximum elevation is 113.5 m above m.s.l., which coincides with the last electrode of the current (Fig. 6a). The first electrode in Line-2 has an elevation of 30.0 m above m.s.l., and the elevation at the subsequent electrodes increases continuously until the last electrode is 70.0 m above m.s.l (Fig. 6b). Meanwhile, in Line-3, the first electrode has an elevation of 41.0 m above m.s.l. and continues to increase with increasing distance between the electrodes until the last electrode is 57.5 m

above m.s.l. (Fig. 6c). Elevation variations on each profile line, as shown in Figs. 6a, 6b, and 6c form a steep slope. Such elevation variations significantly affect the landslide movement at the investigated site (Ayele and Cherie, 2021).

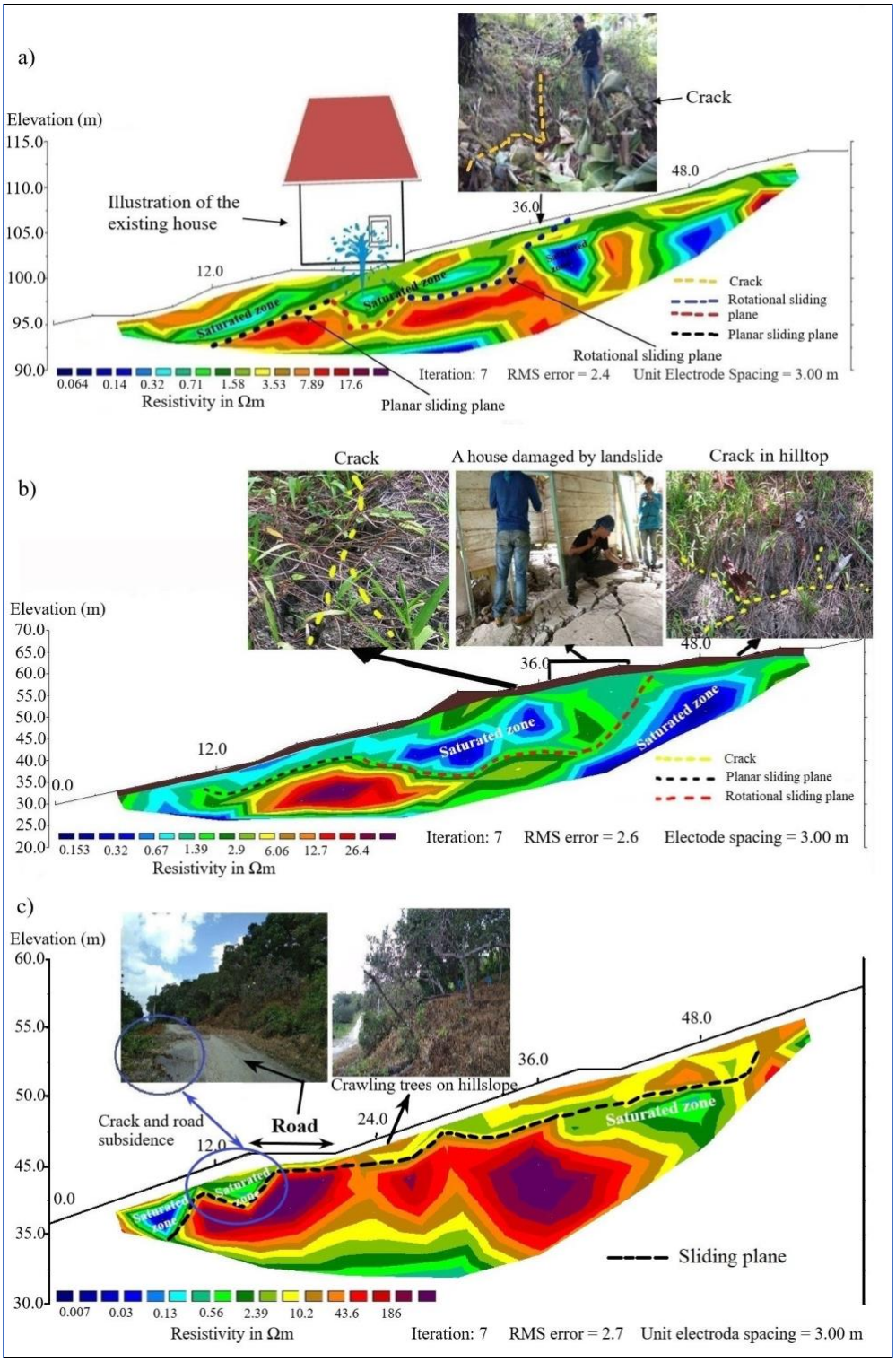


Fig 6. The 2-D ERT sections for Line-1 (a), Line-2 (b), and Line-3 (c) after involving the topographic effect; each section equipped with photographs of its surrounding field conditions.

The 2-D ERT section of Line-1 as presented in Fig. 6a exhibits several zones having resistivity values of <3.0 Ωm, which probably represent the saturated zones. As exhibited in Fig. 6a, the existence

of zones with saturated conditions generally coincides with the presence of cracks above them, which may act as a pathway for rainwater to enter these zones. Just below these saturation zones, a soil layer with resistivity values ranging from 3.0 - 17.6 Ωm may exist that may represent the clay layer. The interface between the saturation zone and the clay layer has an irregular shape, which is a combination of an inclined plane (denoted by the thick black dotted line) and an unevenly curved upward plane (marked by the thick blue and red dotted lines). Such a clay surface combination may act as a sliding surface of landslide, and the type of slide movement that may be generated is a complex (multiple rotational) landslide (Hungr et al., 2013; Schlögel et al., 2015).

Regarding the curved upward plane in Fig. 6a, the thick blue line shows the shape of a symmetrical concave in position about 21- 27 m, while the dotted red line displays a sloping concave at about 27- 39 m of the resistivity line. We do not yet understand the internal mechanism that causes rainwater to re-eject onto the floor of a house (as illustrated at the top of Fig. 6a), but it is possible that the two concave planes played a role in this event.

Fig. 6b displays the 2-D ERT section for Line-2 after involving the topographic effect. The resistivity values of < 3 Ωm are in the near-surface zone along the lateral positions of 6 - 36 m and at the deeper zone along the positions around 36- 51 m. Zones with resistivity values of < 3 Ωm represent saturation zones. The presence of these saturation zones coincides with the existence of cracks at the ground surface just above the saturation zones (as presented at the top of Fig. 6b). The saturation zone in the lateral position of 6- 36 m is overlain by insensitive clay with resistivity values ranging from 3 Ωm to 26.4 Ωm. Meanwhile, the saturation zone in the lateral position of about 36 - 51 m superimposes the topmost clay layer. The interface between the saturated zone (sensitive materials) and the undisturbed clay may act as a sliding surface of the landslide that occurred at the investigated site. As in Line-1, the slip plane shown in Fig. 6b is a combination of a planar (the dotted black line) and uneven curvature (the dotted red line) sliding plane that usually generates complex (multiple rotational) landslides.

The 2-D ERT section for Line-3 is presented in Fig. 6c. There are several saturated zones characterized by resistivity values of < 3 Ωm and an undisturbed zone with resistivity values ranging from 3 Ωm to 186 Ωm. The boundary between the saturation zone and the undisturbed zone (indicated by the dotted black line) may play a role as a sliding plane of landslides in this landslide-prone area. The shape of the slip plane tends to be planar and may generate translational landslides. On the top of Fig. 6c, we also include photographs of crack and road subsidence, as well as crawling trees on the hill slope on the right side of the road. The crack and the road subsidence may be caused by instability in the saturation zones presented on the left shoulder of the road.

In-situ geology surveys were carried out in the areas near ERT profile lines. The slope measurements of the ERT electrode arrays for Line-1, Line-2, and Line-3 using the geology compass of Brunton showed slopes of 34° (or 68%), 20.5° (or 37.4%), and 25.0° (or 46.6%), respectively, in a direction from north to south. This slope is consistent with the depiction shown in Fig. 1. Theoretically, the slope ranging from 16° to 35° (or 30 - 70%) is a steep slope (Van Zuidam, 1985) and has the potential to cause landslides. Such slope magnitudes have a significant role in triggering landslides at investigated sites. The higher the incline, the greater the force required to drive the material mass.

Investigation to the slope morphology (Figs. 7a and c) nearby the profile Line-1 and Line-2 exhibited that the head of displaced material moved almost vertically downward. Moreover, the existing banana trees tilted backward toward the scarp presented nearby the head of displaced material (Fig. 7a). Both situations indicate characteristics of the complex (multiple rotational) landslides. Theoretically, such a landslide is triggered by a combination of planar and curvature sliding planes or by uneven curvature plane (Highland and Bobrowsky, 2008). These slope morphology characteristics confirm the results from the ERT approach.

Observations of soil outcrops around the ERT lines showed the presence of a layer of clay exposed due to a previous landslide (Fig. 7b). This clay layer is most likely to act as a slide plane of the landslide.

The presence of the clay outcrop near this measurement line reinforces the interpretation of the existence of the clay layer from the ERT analysis.

The occurrence of landslides at the investigated location may also be influenced by the distance of the location being very close to the road (Fig. 7d). It even appears that the existing main road was made by cutting the slope, and as a result, it has the potential to destabilize the slope. Therefore, geological and geophysical investigations are essential to be conducted before road and building construction.

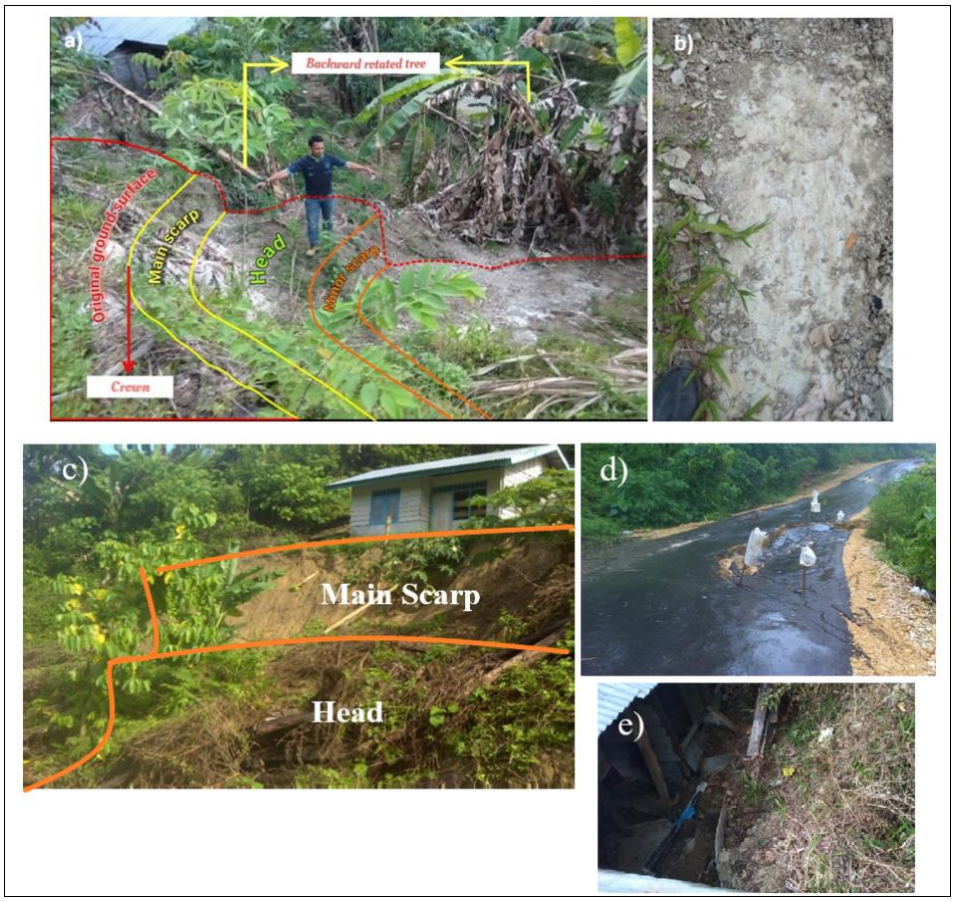


Fig. 7. Slope morphology nearby the profile Line-1 and Line-2 (Figs. 7a and c, respectively); Outcropping of the undisturbed clay layer interpreted as a slip plane (b); Road subsidence nearby the profile Line-3 (d); and a house damaged by the landslide (e).

6. Conclusions

Estimation of ground deformation using the InSAR method shows that the ground materials of the slopes are deformed with a magnitude ranging from -53 mm to +55 mm from the years 2015 to 2017. The negative mark of the magnitude means that the ground deformation is ground subsidence and the positive means ground uplift. This slow deformation of subsidence and the cracking of surficial ground materials on a steep hillside may be the initial potential for landslides.

The ERT method has successfully estimated the existence of the saturated zones, the clay layer that acts as a slip plane, and the shape of the slip surface based on the electrical resistivity value of subsurface layers. There are at least two types of slip planes estimated, namely planar and uneven curvature planes that generate the translational (planar) and complex (multiple rotational) landslides, respectively. The ERT method also provides a good estimate of ground saturation causing road subsidence in the investigated site.

The in-situ geological surveys on the parameters that affect the landslide show that all parameters significantly trigger the landslides, involving the elevation, the slopes ranging from 20.5° to 34°, and the

presence of the undisturbed clay which acts as a slip plane. Slope morphology surveys at the investigated sites indicated the characteristics of complex (multiple rotational) landslides generated by a combination of planar and uneven curvature planes. Therefore, the in-situ geology investigation confirms the results from the InSAR and the ERT approaches.

All parameters investigated from the three approaches above describe the potential for landslides that threaten the study area. Therefore, engineering maintenance actions to remove landslides in the study area are essential to be conducted.

Acknowledgements

We would like to express our gratitude to the Government of North Buton Regency, South East Sulawesi, Indonesia for the funding support in conducting this research. We also thank the students of the Department of Geophysical Engineering of Halu Oleo University for their assistance during the in-situ survey.

References

Ayele, N.A., Cherie, S.G., 2021. Landslide susceptible mapping using InSAR and GIS Techniques: Overview of Debresina Area. Ethiopia. Journal Geological Geophysics, 10, 988.

Bellanova, J., Calamita, G., Giocoli, A., Luongo, R., Perrone, A., Lapenna, V., Piscitelli, S., 2016. Electrical Resistivity Tomography surveys for the geoelectric 2 characterization of the Montaguto landslide (southern Italy). Nat. Hazards Earth System.

Borrelli, L., Antronico, L., Gullà. G., Sorriso-Valvo, G.M., 2014. Geology, geomorphology and dynamics of the 15 February 2010 Maierato landslide (Calabria, Italy). Geomorphology, 208, 50–73.

BPBD North Buton Regency, 2018. Laporan Tahunan Kejadian Bencana Alam Buton Utara, North Buton Regency, Indonesia.

Czikhardt, R., Papco, J. , Bakon, M. , Liscak, P., Ondrejka, P., Zlocha, M., 2017. Ground stability monitoring of undermined and landslide prone areas by means of Sentinel-1 Multi-Temporal InSAR, case study from Slovakia. Geosciences, 7, 87; doi:10.3390/geosciences7030087.

Davidson, J.W., 1991. The Geology and Prospectivity of Buton Island, S.E. Sulawesi Indonesia. Proceeding IPA20th, Jakarta.

Falae, P.O., Kanungo, D.P., Chauhan, P.K.S.,·Dash, R.K., 2019. Electrical resistivity tomography (ERT) based subsurface characterisation of Pakhi Landslide, Garhwal Himalayas, India. Environmental Earth Sciences, 78, 430.

Fattahi, H., 2015. Geodetic imaging of tectonic deformation with InSAR. Ph.D. Thesis, Department of Marine Geology and Geophysics, University of Miami, Florida, USA.

Fressard, O., Maquaire, Y., Thiery, R., Lissak, D.C., 2016. Multi-method Characterisation of an Active Landslide: Case Study in the Pays d'Auge Plateau Göktürkler, G., (Normandy, France). Geomorphology, 270, 22–39.

Galli, M., Guzzetti, F., 2007. Landslide vulnerability criteria: a case study from umbria, central Italy. Environmental Management, 40**,** 649–665 .

Giocoli, A., Stabile, T. A., Adurno, I., Perrone, A., Gallipoli, M.R., Gueguen, E., Norelli, E., Piscitelli S., 2015. Geological and Geophysical Characterization of the Southeastern Side of the High Agri Valley (Southern Apennines, Italy). Nat. Hazards Earth System. 15, 315–323.

Highland, L., Bobrowsky, P.T., 2008. The Landslide Handbook: A Guide To Understanding Landslides. US Geological Survey, Reston, VA, USA, 129.

Hu, Z., Shan, W., 2016. Landslide investigations in the northwest section of the lesser Khingan range in China using combined HDR and GPR methods. Bulltein Engineering Geology Environment, **75,** 591–603.

Hungr, O., Leroueil, S., Picarelli, L., 2013. The Varnes classification of landslide types, an update. Springer-Verlag Berlin Heidelberg.

Jaya, L.M.G., Safani, J., Okto, A., Hasbi, M., Kadir, A., 2020. Ground deformation analysis on road infrastructure in North Buton Indonesia using Interferometric Synthetic Apertur Radar (InSAR), Conf. Series: Earth and Rnvironmental Science 419, 012095.

Jongmans, D., Bievre, G., Renalier, F., Schwartz, S., Beaurez, N., Orengo, Y., 2009. Geophysical investigation of large landslide in glaciolacustrine clays in the Trieves area (French Alps). Engineering Geology, 109 (1-2), 45-56.

Kannaujiya, S., Chattoraj, S.L., Jayalath, D., Ray, P.K.C., Bajaj, K., Podali, S., Bisht, M. P. S., 2019. Integration of satellite remote sensing and geophysical techniques (electrical resistivity tomography and ground penetrating radar) for landslide characterization at Kunjethi (Kalimath), Garhwal Himalaya, India. Natural Hazards: Journal of the International Society for the Prevention and Mitigation of Natural Hazards, 97, (3), 12.

Lievens, H., Verhoest, N.E.C., De Keyser, E., Vernieuwe, H., Matgen, P., Álvarez-Mozos, J., De Baets, B., 2011. Effective roughness modeling as a tool for soil moisture retrieval from C- and L-band SAR. Hydrology Earth System Science, 15, 151–162.

Loke, M.H., 2020. Tutorial: 2-D and 3-D electrical imaging surveys.

Murdzek, R., Malik, H., Leśniak, A., 2018. The use of the DInSAR method in the monitoring of road damage caused by mining activities, E3S Web of Conferences 36 02005.

Necula, N., Niculita, M., Fiaschi, S., Genevois, R., Riccardi, P., Floris, M., 2021. Assessing urban landslide dynamics through multi-temporal InSAR techniques and slope numerical modeling. Remote Sensing, 13, 3862.

Perrone, A., Zeni, G., Piscitelli, S., Pepe, A., Loperte, A., Lapenna, V., Lanari, R., 2006. Joint analysis of SAR interferometry and electrical resistivity tomography surveys for investigating ground deformation: the case-study of Satriano di Lucania (Potenza, Italy). Engineering Geology, 88 (3-4), 260-273.

Rauff, K.O., Abir, I.A., Perissin, D., 2020. Characterisation of landslide using InSAR technique and electrical resistivity method at Paya Terubong, Malaysia. Journal Indian Society, Remote Sensing, 48, 1223–1236.

Schlogel, R., Doubre, C.., Malet, J-P., Masson, F., 2015. Landslide deformation monitoring with ALOS/PALSAR imagery: A D-InSAR geomorphological interpretation method. Geomorphology, 231, 314–330.

Sikumbang, N., Sanyoto, P., Supandjono, R.J.B., Gafoer, S., 1995. Peta Geologi Lembar Buton, Sulawesi, skala 1:250.000. Pusat Penelitian dan Pengembangan Geologi, Bandung.

Szalai, S., Prácser, E., Szokoli, K., Tóth, Á., 2017. Prediction of the Process of a Slowly Moving Loess Landslide by Electrical Resistivity Tomography. In: Mikoš, M., Arbanas, Ž., Yin, Y., Sassa, K. (eds) Advancing Culture of Living with Landslides. WLF 2017, Springer, Cham.

Tuncel, A., Kincal, C., Berge, M.A., 2021. Site investigation of a landslidesite and its surroundings: a case study at Egridere district, Northern Izmir city, Turkey. Arabian Journal of Geosciences, 14, 2108.

Uhlemann, S., Wilkinson, P.B., Chambers, J.E., Maurer, H., Merritt, A.J., Gunn, D.A., Meldrum, P.I., 2015. Interpolation of landslide movements to improve the accuracy of 4D geoelectrical monitoring. Journal Applied Geophysics, 121, 93-105.

Varnes, D.J., 1978. Slope movement types and processes, Transportation Research Board Special Report, 176.

Virk, A.S., Singh, A., Mittal, S.K., 2018. Advanced MT-InSAR Landslide Monitoring: Methods and Trends. Journal Remote Sensing, GIS, 7, 1.

Wang, G., Furuya, G., Doi, I., Watanabe, N., Wakai, A., Marui, H., 2015. Investigation on the internal structure of Higashi-Takezawa Landslide dam using surface wave method and micro-tremor array measurement. Journal of the Japan Landslide Society, 52(5), 233–238.

Yan, Y., Yan, Y., Zhao, G., Zhou, Y., Wang, Z., 2022. Combined ERT and GPR data for subsurface characterization of weathered hilly slope: a case study in Zhejiang Province, Southeast China. Sustainability, 14, 7616.

Zhou, C., Gong, H., Chen, B., Li, J., Gao, M., Zhu, F., Chen, W., Liang, Y., 2017. InSAR time-series analysis of land subsidence under different land use types in the Eastern Beijing Plain, China. Remote Sensing, 9(4), 380.

Van Zuidam, R.A., 1985. Aerial Photointerpretation in Terrain Analysis and Geomorphologic Mapping. The Hague: Smits, The Netherlands, 442.